OPTIMISATION TECHNIQUE FOR ARC WELDING OF STRUCTURED SHEET

IVANOV Sergei[1], KARKHIN Victor[1], PANCHENKO Oleg[2], MICHAILOV Vesselin [2]

[1] The Peter the Great St.Petersburg Polytechnic University, Russia
[2]Brandenburg University of Technology, Cottbus, Germany

Abstract

Effects of weld path curvature on microstructure and mechanical properties of structured sheet arc welded joints are studied. Solution of the direct heat conduction problem is obtained by the Green's function method. Optimisation problem for obtaining a constant weld or heat affected zone width is formulated and solved numerically. The optimum power distribution along the curved weld path in arc welding of a 0.7 mm thick steel panel is presented.

Keywords: arc welding, structured sheet, microstructure, hardness, temperature field, optimisation.

1. INTRODUCTION

Stiffness of sheet structures can be increased by the formation of cell structured surface on it. Welding along the cell boundaries leads to formation of curved weld with recognizable non-uniformity of bead width and heat affected zone (HAZ) (Fig. 1). In this case selection of welding parameters rise to solution of the following optimization problem: to find such parameters of heating technology which provide the given geometry of heated zone and/or product properties. Required (variable) parameters of heating technology can have different nature (power distribution of heat source, its speed, path, etc.) [1, 2]. Features of heating processes and ability of welding parameters optimization of joint with curved welds is not studied enough.

The aim of study is to develop the procedure for optimisation of arc welding parameters of structured sheet metal.

2. EXPERIMENTAL PROCEDURE

Arc welding of structured sheet from low carbon steel DC04 (≤0.08% C and ≤0.4% Mn) with thickness h = 0.7 mm (fig. 1) was studied. Steel thermophysical properties: thermal conductivity λ = 0.025 W mm-1 K-1, thermal diffusivity a = 5 mm2 s-1, melting temperature Tm = 1728 K. Welding procedure: current I = 45 A, voltage U = 10.5 V, welding speed v = 15 mm s-1, filler wire G2Si1 (0.07% C, 1.0% Mn, 0.3% Si) diameter 0.8 mm, shielding gas 82% Ar + 18% CO2, initial temperature To = 293 K [3].The structured sheets with structure width of 33 mm, structure height of 3 mm and bend radius of 5 mm are considerably increase stiffness and decrease aerodynamic drag [4]. Arc movement along the cell boundaries with constant speed and power (constant heat input) and variable bend radius leads to formation of curved weld with recognizable asymmetry of temperature field about arc trajectory (non-uniformity of bead width and HAZ) (fig. 1). It leads to inhomogeneity of microstructure and mechanical properties along the weld.

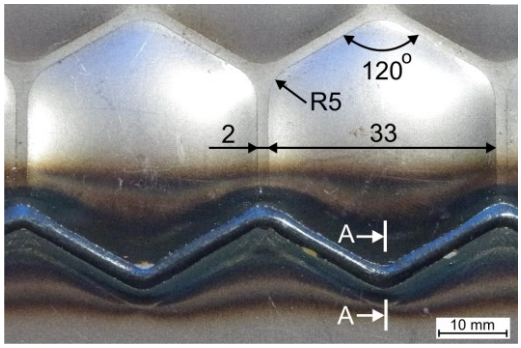

Fig. 1 Overview of GMA welded joint of structured sheet with thickness 0.7 mm.

3. MICROSTRUCTURE AND PROPERTIES OF WELDED JOINT

Varied width of HAZ and its components (coarse grain HAZ (CGHAZ), fine grain HAZ (FCHAZ), inter-critical HAZ (ICHAZ), sub-critical HAZ (SCHAZ)) is the result of asymmetrical temperature field (fig. 2). Hardness distribution measured in central plane of the sheet provides the overview of inhomogeneity of local mechanical properties in the weld (fig. 2a). An elevated HAZ hardness can be explained by formation of non-equilibrium microstructure under high cooling rate (cooling time in the range 1123 - 773 K of the metal heated up to T_{max} = 1625 K $\Delta t_{8.5/5}$ =8.5 s for left wide part of HAZ and 6.5 s for right narrow part of HAZ).

Base metal consists mostly of ferrite and a small amount of perlite. An anisotropy of mechanical properties is determined by stretching of ferrite grains along the rolling direction. Usage of filler wire with chemical composition different from base metal leads to formation of welding bead with consists of acicular ferrite with interlayers of polygonal and Widmanstatten ferrite along the former austenite grain boundaries. Low cooling rate promotes formation of pronounced CGHAZ comprised of mixture of quasipolygonal and Widmanstatten ferrite. FCHAZ contains equiaxial grains of polygonal ferrite with almost identical diameter.

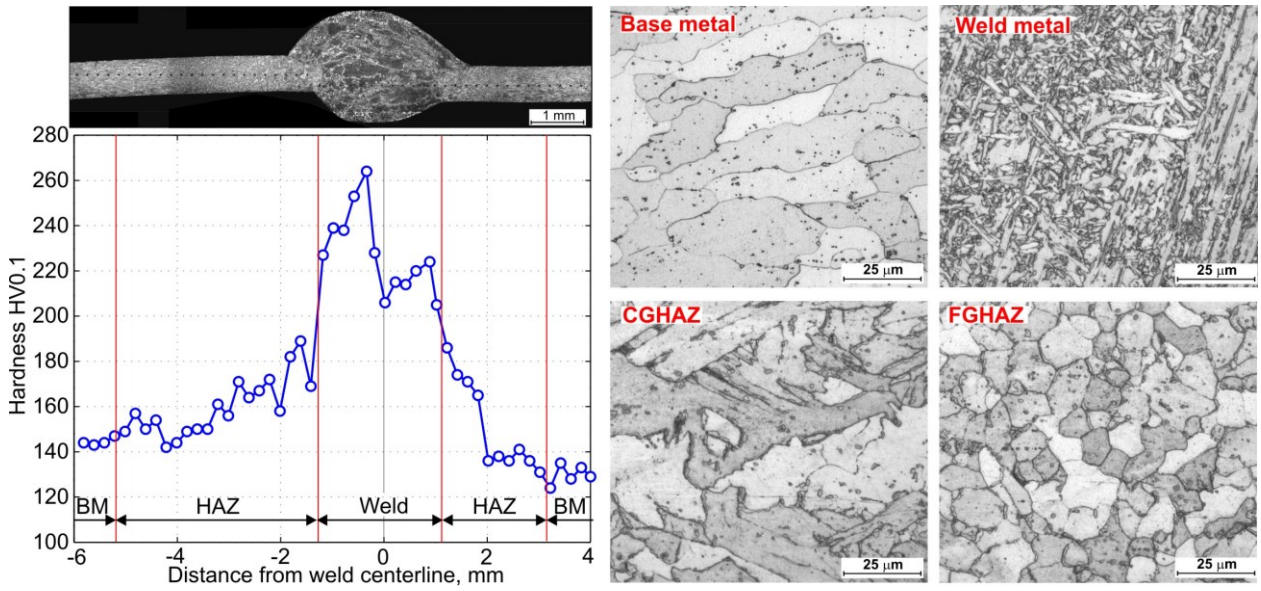

a) b)

Fig. 2 Microhardness distribution (a) and microstructure (b) in section A-A of welded joint (see. fig. 1).

4. SOLUTION OF DIRECT HEAT CONDUCTION PROBLEM

During solution of direct heat conduction problem welded sheets is represented as a solid layer (curvature of surface was neglected) and welding arc is normally distributed surface heat source. Heat flow distribution can be described by equation:

$$q_2(r) = \frac{q}{\pi r_e^2} \exp\left(-\left(r / r_e \right)^2 \right), \tag{1}$$

where r is a distance to heat source axis, r_e is normal radius of heat source (distance to the center of heat source, on which power decreases in e ≈ 2.72 times). Heat source net power $q = \eta_h UI = 0.9 \times 10.5 \times 45 = 425.25$ W (where arc thermal efficiency $\eta_h = 0.9$ [5]) radius $r_e = 2$ mm.

Assume that the continuous heat source moves on the surface of flat layer with given trajectory ABCD and at the moment t it situated in point C (Fig. 3a). Let us find the temperature field by the Green's function method. Consider the continuous source as a complex of instantaneous elementary sources, which is situated in point B with coordinates $(\xi,\eta,0)$ and act at the moment τ during $d\tau$ and release energy $q(\tau)d\tau$. Then temperature increment from elementary source in any point $P(x,y,z)$ in the moment t can be described by following equation [2]:

$$dT(x,y,z,t) = \frac{q(\tau)d\tau / h}{4\pi\lambda(t-\tau+t_0)} \exp\left(-\frac{[x-\xi(\tau)]^2 + [y-\eta(\tau)]^2}{4a(t-\tau+t_0)} \right) \times$$

$$\times \left[1 + 2\sum_{i=1}^{\infty} \cos\left(\frac{\pi i z}{h} \right) \exp\left(-\pi^2 i^2 \frac{a(t-\tau)}{h^2} \right) \right], \tag{2}$$

where $t_0 = r_e^2/(4a)$, $(t-\tau)$ - is time of elementary source heat passage.

Summarize heat increment from all elementary sources (integration of the equation (2) over t) gives

$$T(x,y,z,t) - T_0 = \frac{q/h}{4\pi\lambda} \int_0^{\min(t,t_f)} \frac{1}{t-\tau+t_0} \exp\left(-\frac{[x-\xi(\tau)]^2 + [y-\eta(\tau)]^2}{4a(t-\tau+t_0)} \right) \times$$

$$\times \left[1 + 2\sum_{i=1}^{\infty} \cos\left(\frac{\pi i z}{h} \right) \exp\left(-\pi^2 i^2 \frac{a(t-\tau)}{h^2} \right) \right] d\tau, \tag{3}$$

where t_f is expiration time of heat source in point D (fig. 2). It is not complicate to find the integral numerically because of known trajectory ($\xi(\tau)$ and $\eta(\tau)$ is specified functions). All characteristics of temperature field (maximum temperature field, thermal cycles, cooling rate, etc.) can be calculated by equation (3).

Maximum temperature field far from weld beginning is shown in fig 3b. It's asymmetrical relative to curvilinear trajectory especially at transition region between two linear parts of weld. Such temperature distribution is confirmed experimentally (see fig. 1).

During welding along curved path the field of heat flow is more complicated than during linear welding. It affects on thermal cycles (fig. 4a). It is seen that curves are intersecting. For example temperature in point 1 more distant from arc axis is higher than in closer point 3. Results of calculation are in good agreement with experiment.

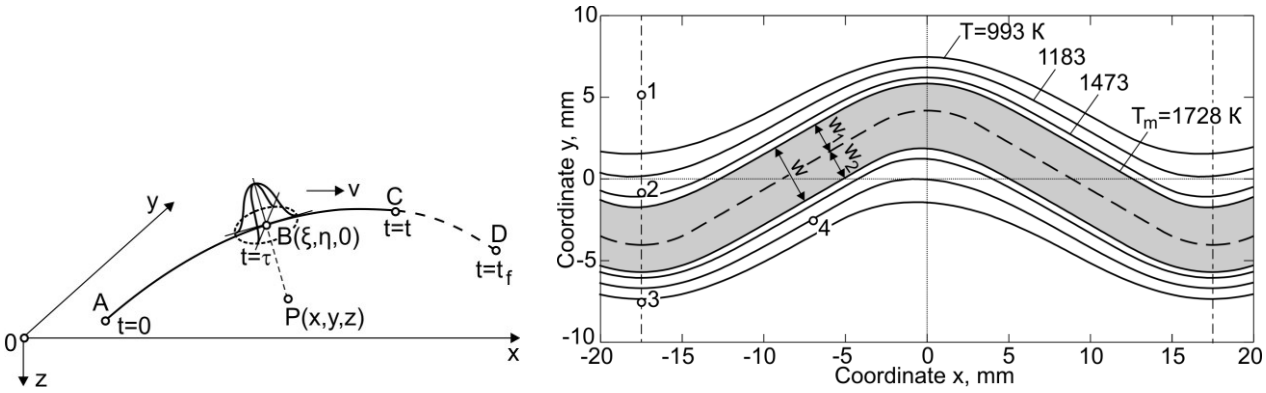

a) b)

Fig. 3 Schematic of calculation of temperature in point P (a) and calculated maximum temperature field on the surface of welded joint (welding trajectory is presented by dashed line).

If arc power q and welding speed v is constant than half-width W1 and W2 and total width W ($W=W_1+W_2$) is vary along weld (fig. 4b). Weld bead boundaries (isotherms $T_{max} = T_m$) has a different distance from arc path.

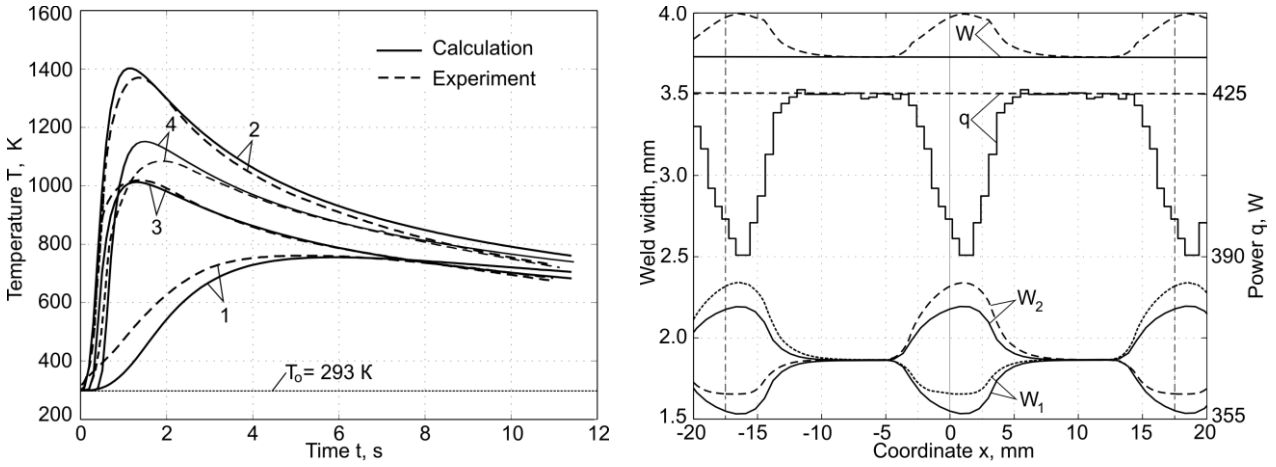

a) b)

Fig. 4 Thermal cycles during welding with constant arc power (points 1 – 4 are shown in fig.3) (a) and distribution of weld width and arc power along curved weld at constant power (dashed and dotted lines) and at optimal power (solid line) (b).

5. SOLUTION OF OPTIMIZATION PROBLEM

An optimum criterion is commonly called objective function. For welding and allied processes it can be formulated using a least-squares deviation method [6-8]:

$$F(\mathbf{p}) = \sum_{j=1}^{J} w_j^f [f_j^m - f_j(\mathbf{p})]^2 + \sum_{k=1}^{K} w_k^p [p_k^0 - p_k]^2 + R.T. \rightarrow \min ; \quad (4)$$

$$p_{k\ \min} < p_k < p_{k\ \max},$$

where **p** is unknown parameter vector, **p** = {p_1, p_2,… , p_K}; J is number of observations; K is number of unknown parameter; f_j and f_j^m is calculated and measured value of weld characteristic at point j; p_k and p_k^0 – unknown parameter and its prescribed value, w_j^f and w_k^p is the weighting factor for temperature field characteristic in jth point and kth required parameter; *R.T.* – regularization element.

For example welding cross section size (distance between melting isotherm, HAZ width and crater geometry), time and cooling rate in temperature interval other characteristics of heat processes can be taken as a response function f. Weighting factors are defined by investigator. Regularization permits to smooth over the required function of power distribution. The given p_k^0 value kth parameter may include limitations with value ($p_{k\ \min}$, $p_{k\ \max}$). To be accented that objective function determination is the most important step in formulation of optimization problem. It is affected with investigator that's why it is subjective. Solving of optimisation problem relatively to unknown parameters (inverse problem) resolve into repeated direct problem analytical or numerical solving.

Now let us obtain constant weld, W= W_1+W_2=const (constant distance between isotherms $T_{\max}$ = T_m on the face surface) by varying of arc power q at a constant welding speed v. Then the objective function (4) can be presented in a simplified form:

$$F(\mathbf{q}) = \sum_{j=1}^{J} [W_j^m - W_j(\mathbf{q})]^2 \rightarrow min, \tag{5}$$

where J – amount of target weld path sections where weld width W is determined. Contribution of each section is equal (all weighting coefficients is identical).

Let us find the optimal power distribution along the weld. One section of the weld in the range 0 - 17.5 mm along the x axis divide on J transversal sections (fig. 5). Corresponded travel time of heat source t_{int} = 1.3 s divide on K equal steps. Assume that heat source power is equal in the each k time step, q_k = const. Then solution of equation (5) relative to desired vector **q** with components q_1, q_2,…, q_K can be obtained by the well-known optimization methods.

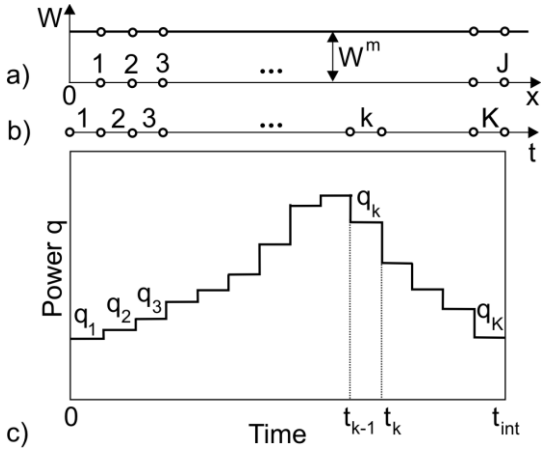

Fig. 5 Optimisation problem for heat input: a - required weld width and numeration of controlled sections along weld axis; b - numeration of time steps; c - power distribution during welding.

Optimal power distribution along weld was obtained by steepest descent method with K = J = 30 (fig. 4b). It is seen that the power reduces in the junction between two straight sections of the weld. Weld with constant width W = 3.73 mm refers to such power distribution. Corresponded half-widths W_1 and W_2 are unequal as a HAZ width astride the weld.

CONCLUSION

1. The proposed optimisation technique of welding conditions of curvied welds considers the main arc welding parameters, properties of welded material and joint geometry. The technique is based on offered objective function and on analytical solution of corresponding heat conduction problem.

2. The curved weld with constant width can be obtained by optimal distribution of arc power along the weld at constant welding speed.

ACKNOWLEDGEMENTS

The research has been performed at the Peter the Great St. Petersburg Polytechnic University under the contract № 14.Z50.31.0018 with the Ministry of Education and Science of the Russian Federation)

REFERENCES

[1] Kondoh K., Ohji T. Algorithm based on non-linear programming method for optimum heat input control in arc welding. Science and Technology of Welding and Joining, Vol.3, №3. 1998, pp. 127-134.

[2] Karkhin V.A. Thermal processes in welding. St. Petersburg State Polytechnic University, 2013. 646 p (in Russian).

[3] Schleuss L., Springer K., Zoeke J., Ossenbrink R., Michailov V. Qualifizierung von warmearmen MSG-Schweissverfahren fur Leichtbaukonstruktionen mit strukturierten Halbzeugen. Join Ex Kongress, 10-11 Okt. 2012, Wien.

[4] Malikov V., Ossenbrink R., Viehweger B., Michailov V. Experimental study of the change of stiffness properties during deep drawing of structured sheet metal. Journal of Materials Processing Technology, Vol.213, №11, 2013, pp. 1811-1817.

[5] Pepe N., Egerland S., Colegrove P., Yapp D. Leonhartsberger A., Scotti, A. Measuring the process efficiency of controlled gas metal arc welding processes. Science and Technology of Welding and Joining., Vol.16, №5, 2011, pp. 412-417.

[6] Karkhin V.A., Levchenko A.M. Computer-aided determination of diffusible hydrogen in deposited weld metal, Welding in the World, Vol. 52, №3/4, 2008, pp. 3-11.

[7] Karkhin V.A., Plochikhine V.V., Bergmann H.W. Solution of inverse heat conduction problem for determining heat input, weld shape, and grain structure during laser welding. Science and Technology of Welding and Joining, Vol.7, №4, 2002, pp. 224-231.

[8] Karkhin V.A., Plochikhine V.V., Ilyin A.S., Bergmann H.W. Inverse modelling of fusion welding processes. Welding in the World, Vol.46, №11/12, 2002, pp. 2-13.